Astron. Astrophys. 171, 305–316 (1987)

ASTRONOMY
AND
ASTROPHYSICS

Center-to-limb variation of Stokes profiles and the diagnostics of solar magnetic fluxtubes

J.O. Stenflo[1,★], S.K. Solanki[1,★], and J.W. Harvey[2]

[1] Institute of Astronomy, ETH-Zentrum, CH-8092 Zürich, Switzerland
[2] National Solar Observatory★★, P.O. Box 26732, Tucson, AZ 85726, USA

Received May 12, accepted June 3, 1986

Summary. Simultaneous recordings of the Stokes I, Q, and V spectra have been performed with a Fourier transform spectrometer in 10 solar regions distributed over various center-to-limb distances, from disk center to the extreme limb. The observational material and the recording technique used are presented. We then evaluate the Stokes profile parameters for a small selected set of spectral lines to explore the potential of this qualitatively new data set for the diagnostics of spatially unresolved magnetic fluxtubes.

The center-to-limb variations of different Stokes line-ratio parameters as well as the asymmetry between the σ and π components of the Stokes Q profile provide information on the decrease of the fluxtube kG field strength with height in the atmosphere. The "thermal" line ratios suggest that the temperature difference between fluxtube interior and exterior at equal optical depth *decreases* with height. The center-to-limb variations of the Stokes V asymmetries contain information on the geometry of the mass motions in the fluxtube interiors. The absence of any Doppler shift of the Stokes V zero-crossing wavelength for any limb distance gives evidence that these mass motions cannot be represented by quasi-stationary flows.

Key words: solar magnetic fields – fluxtubes – Stokes parameters – line profiles

1. Introduction

As the basic photospheric magnetic flux elements on the sun cannot be spatially resolved with existing instrumentation, spectral techniques have to be used to overcome the spatial resolution limit to determine the physical conditions inside the magnetic fluxtubes. The line-ratio method (Stenflo, 1973, 1976) for instance made it possible to conclude that more than 90% of the total flux seen in magnetograms occurs in kG form, although the apparent field strengths seen in quiet regions are generally much smaller due to the large amount of spatial smearing of the small, subarcsec magnetic structures caused by seeing and the instrument. At the end of the 1970s a breakthrough for the diagnostics of the spatially unresolved fluxtubes occurred with the development of the Fourier transform spectrometer (FTS) of the McMath telescope at the National Solar Observatory (Kitt Peak) into a Stokes polarimeter (Brault, 1978; Stenflo et al., 1984).

The FTS combines broad simultaneous spectral coverage (typically 1000 Å) with superior spectral resolution (no significant instrumental broadening) and insignificant straylight. The recorded spectra can therefore be regarded as being free from instrumental effects apart from smearing due to spatial and time integration. It should be remembered that the magnetic structures are greatly spatially smeared by any other approach as well, but these other methods do not have the spectral advantages of the FTS. Since many hundreds of fully resolved Stokes line profiles are recorded strictly simultaneously, and since these various lines respond differently to the physical conditions in the spatially unresolved magnetic fluxtubes, depending on their Landé factors, line strengths, excitation potentials, etc., an intercomparison between the Stokes profiles provides a wealth of diagnostic information on the fluxtube interiors. The diagnostic contents of the FTS Stokes spectra for fluxtube modelling have been described in Stenflo et al. (1984). Stenflo and Harvey (1985) analysed Stokes I and V spectra of the Fe I $\lambda\lambda$ 5247.06 and 5250.22 Å lines obtained with the FTS and with a grating spectrometer and found indications of large mass motions inside the fluxtubes (from the Stokes V asymmetries) but no systematic downdrafts (no significant Doppler shift of the Stokes V zero-crossing wavelength), in contrast to previous investigations with lower spectral resolution. It has been shown (Solanki and Stenflo, 1986) that the apparent downdrafts previously reported can in fact be explained as an effect of the limited spectral resolution of these earlier studies.

To make more complete use of the diagnostic potential of the FTS Stokes spectra Solanki and Stenflo (1984, 1985) applied and extended the statistical approach introduced by Stenflo and Lindegren (1977) to analyse the behavior of simultaneously recorded Stokes V profiles of a large number of unblended lines: 400 Fe I and 50 Fe II lines. This allowed the construction of models of the temperature structure of the fluxtube interior (Solanki, 1984), substantially different from previous models (called "facular" models in traditional terminology). Most of this discrepancy is due to the circumstance that previous facular models have largely been based on Stokes I information alone, which is greatly contaminated by contributions from the fluxtube surroundings, since the fluxtubes are never (except possibly for sunspots) spatially resolved. In contrast, the contributions to the

Send offprint requests to: J.O. Stenflo
★ Visiting astronomer, National Solar Observatory
★★ Operated by the Association of Universities for Research in Astronomy, Inc., under contract with the National Science Foundation

Stokes V profiles come exclusively from the fluxtube interiors. This is where the remarkable diagnostic advantage of the *polarized* spectra lies. The statistical approach could also be used to derive extensive information on the dynamics of the fluxtube interiors, which involves mass motions of large amplitude (Solanki, 1986). Reviews of these recent developments have been given by Stenflo (1984, 1985b, 1986).

The investigations described however only represent the first steps in the exploitation of the FTS Stokes polarimeters for fluxtube diagnostics. The FTS recordings used were limited to a few features near disk center. Only two (I and V) of the four Stokes parameters were recorded, over about 2000 Å in the visible spectrum. This demonstrates that the use of the FTS polarimeter is still in its infancy.

In May 1984 we made a new set of observations with the FTS polarimeter with the aim of not only extending previous work, but also introducing qualitatively new dimensions to the problem of fluxtube diagnostics. In comparison with the previous FTS data, the new observations contain the following new features:

(1) The spectra of three Stokes parameters, I, Q, and V, were recorded simultaneously. Thus the transverse Zeeman effect can be incorporated in the fluxtube diagnostics.

(2) Recordings were made over a number of different μ values, to obtain the center-to-limb variations of the Stokes spectra.

(3) Recordings in the infrared, around 1.5 μm, were made in addition to the recordings in the green portion of the spectrum.

The aim of the present paper is to describe the new diagnostic possibilities offered by including the center-to-limb variation and Stokes Q in the analysis. We will illustrate these possibilities by evaluating the properties of the Stokes line profiles of the line pair Fe I $\lambda\lambda$ 5247.06 and 5250.22 Å (which has formed the basis for the line ratio technique in the past) and of two adjacent lines (Cr I λ 5247.57 Å and Fe I λ 5250.65 Å). The analysis of the infrared recordings and the application of a statistical approach to the new data set will be the subject of subsequent investigations. A preliminary presentation of some of the data has already been made in reviews by Stenflo (1985b, 1986).

2. Observations

The FTS observations of the center-to-limb variation of the Stokes I, Q, and V spectra were carried out on May 3–7, 1984, at the McMath telescope of the National Solar Observatory. During the first three days a prefilter selecting the spectral range 4880–6000 Å was used. It is these data that we will consider in the present paper. The last two days were used for similar Stokes I, Q, and V recordings in the near infrared range of 1.47–1.80 μm.

The entrance aperture of the FTS was circular with a diameter corresponding to 5 sec of arc on the sun. We need a relatively large entrance hole both to reduce seeing noise, and to obtain a better signal-to-noise ratio. As the sizes of the magnetic fluxtubes are far smaller than one sec of arc (probably typically of the order of 0.1 sec of arc), they are in any case completely spatially smeared, even if a small aperture of say 0.5 sec of arc could be used. However, as it is much more difficult to keep the magnetic features within the aperture during the integration time (due to seeing, differential rotation and proper motions) when a small aperture is used, it is wiser to work with a larger aperture. However, when observing close to the limb, a large aperture would give a poor μ resolution. For this reason we used the smaller size of 5 sec of arc instead of the 10 sec of arc used in the previous FTS recordings (Stenflo et al., 1984).

For all the 4880–6000 Å recordings the spectral resolution used was 524 000. With an FTS the modulation transfer function is unity out to this value (in contrast to grating spectrometers), so that the solar spectrum is fully resolved, i.e., there is no significant instrumental broadening. The time needed to perform one scan of the interferogram to obtain this resolution was 7.2 min. Note that all the wavelengths within the prefilter range contribute simultaneously to the interferogram during the scan of the path length differences, so the same time integration window applies to all spectral lines recorded. However, different Fourier components that comprise line profiles are sampled at different times, which could cause a systematic distortion of all similar line profiles in a single scan. To enhance the signal-to-noise ratio and reduce systematic line profile distortions the scans were repeated and added. The number of interferogram scans used for each disk position varied between 6 and 10 in our observations. Thus the effective time integration was between 43 min and 72 min (the latter was only used for the position closest to the solar limb).

The recordings in the 4880–6000 Å spectral band were made at 8 different disk positions, distributed over various limb distances (μ = 0.83, 0.67, 0.57, 0.45, 0.30, 0.28, 0.16, and 0.10). The positions were selected by first centering the FTS aperture on a local extremum in the Stokes V signal and then guiding on this point, taking into account the law of differential rotation for photospheric magnetic fields. When searching for a suitable feature, the FTS was set at a fixed path length difference ($\sim$2 cm, corresponding roughly to the inverse of the typical width of solar spectral lines), and the Stokes V signal was monitored on a meter. Only positions with a clearly visually discernible V signal were selected, on which it was possible to properly center the aperture. Areas of closely mixed polarities were avoided. Since the V signal decreases towards the limb due to projection effects (V is proportional to the line-of-sight component of the magnetic flux, whereas the actual direction is expected to be on the average vertical), this procedure favors the selection of stronger magnetic features when going closer to the limb in order to see a signal by eye. Also it favors the selection of magnetic fields inclined towards the observer rather than "typical" magnetic features (which usually have a radial direction out from the sun). Although this selection procedure thus has drawbacks, it seems to be the best alternative for an exploratory investigation, when only a small number of spatial positions on the sun can be sampled (for reasons of time and masses of data; each recording represents a spectral atlas of $\sim 10^6$ samples in three Stokes parameters). Thus the positions close to the limb were selected in strong plages of active-region complexes near the west limb of the sun. By careful inspection of the solar image visible pores in the observed regions were avoided.

To the new set of 8 different disk positions we have added two previous FTS recordings at μ = 1.00 and 0.92, which contain the four lines of interest. They were obtained on April 29–30, 1979 (Stenflo et al., 1984). The full set used thus comprises 10 recordings, distributed in μ from 1.00 (disk center) to 0.10 (5 sec of arc from the limb).

The Stokes V signal, represented by $V_{\mathrm{max},\,5250}$, for the 10 different solar regions sampled is shown in Fig. 1. $V_{\mathrm{max},\,5250}$ is the average of the polarization amplitudes in the blue and red wings of the Fe I λ 5250.22 Å line. Disregarding the problem of

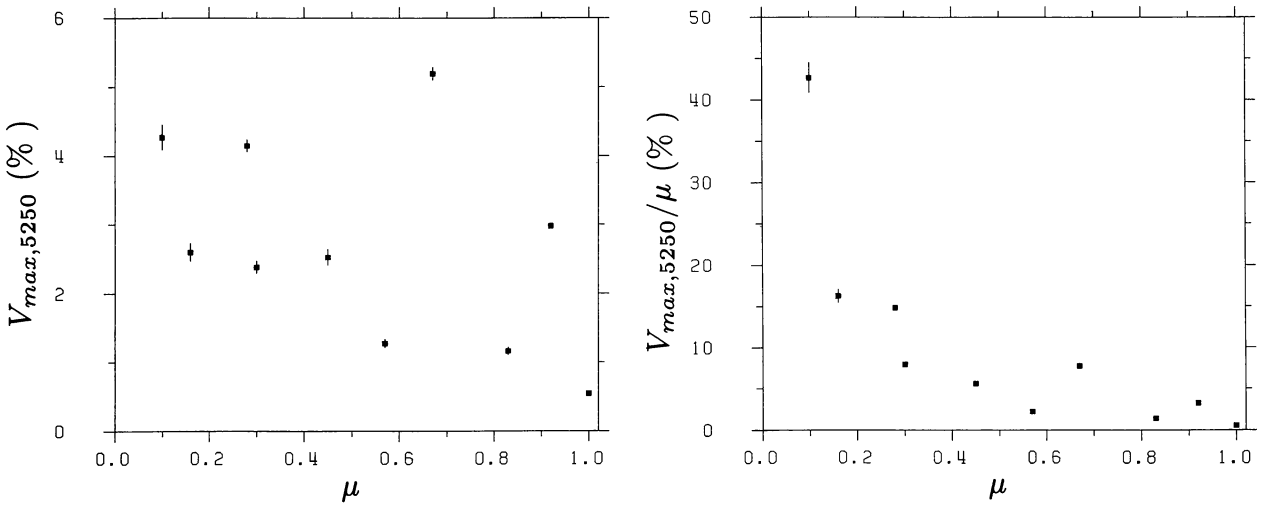

Fig. 1. Polarization signal $V_{\max,5250}$ in the ten observed solar regions, as a function of μ, the cosine of the heliocentric angle. If the true field direction were parallel to the solar radius and field strength constant with height, $V_{\max,5250}/\mu$ would be proportional to the magnetic filling factor

field inclination, this quantity is approximately proportional to the filling factor (fraction of the spatial resolution element covered by magnetic fields), since the intrinsic field strength in the fluxtubes varies little with $V_{\max,5250}$ (Stenflo and Harvey, 1985).

If the true direction of the field in the selected regions were radial and the field strength remained constant with height, then the filling factor would be approximately proportional to the quantity $V_{\max,5250}/\mu$, shown in the right diagram of Fig. 1. Here the two selection effects just mentioned are clearly seen: Stronger magnetic features with more flux (larger filling factors) have been selected when approaching the limb. The very high value of $V_{\max,5250}/\mu$ for $\mu = 0.10$ (merely 5 sec of arc from the very limb) suggests that either a sunspot had been selected by mistake (none was visible to the eye when inspecting the image at this position), or that the magnetic field was strongly tilted away from the radial direction towards the observer, or both. As will be seen from Fig. 8 below, there is strong evidence from the observed Q/V ratio that indeed the tilt away from the vertical direction towards the observer increases when approaching the limb, as a result of our selection procedure. Fortunately the diagnostic problems and the results that will be described in the present paper do not seem to be affected very much by the actual inclination of the magnetic fluxtubes. On the other hand there is a significant dependence on filling factor, which generally increases towards the limb due to the mentioned selection effects.

Although the dependence of field strength on filling factor α is significant, it is relatively small (Stenflo and Harvey, 1985), and it is the center-to-limb variation (μ dependence) that dominates in the present data. The μ dependence arises because the height of formation of the spectrum increases with decreasing μ, and the magnetic field and thermodynamic parameters inside the fluxtubes vary rapidly with height. To fully separate the effects of α and μ, one would need observations that are much more representatively distributed in the $\mu - \alpha$ plane than our present observations are, which may be a challenging goal to achieve in future observations. For our present exploratory investigation, these limitations are however not critical.

After this summary of the properties of the data set, let us outline the instrumental technique used to make the recordings. Instead of using KD*P Pockels cell modulation as in the previous FTS recordings (Stenflo et al., 1984), piezoelastic modulation of the polarization was employed. Thus Stokes V was modulated at the basic resonance frequency of $\nu_V = 20.1$ kHz, while Stokes Q was simultaneously modulated at the second harmonic ($\nu_Q = 40.2$ kHz). The modulation amplitude was set at $\lambda/2.62$, which prevents infiltration of Stokes Q into the DC signal (used for Stokes I) at the intensity-weighted, mean wavelength observed. This setting was made by requiring no variations in the DC signal when turning a Glan-Thompson prism in front of the FTS aperture. Future modifications will allow Stokes U to be recorded as well.

The McMath FTS is sampled at a frequency of 2.5 kHz. Path difference is varied at a rate so that the spectral intensities cause an amplitude modulation of the sampling signal, such that the wavelengths are mapped into audio frequencies, around 833–1250 Hz. The procedure is now to map the Stokes Q and V spectra into separate free portions of the remaining frequency range (0–833 Hz) available to the A/D converter.

The convolution of the piezoelastic modulation frequencies with the audio frequencies generated by the sampling of the interferogram causes the Stokes Q and V spectra to appear at frequencies $\nu_{Q,V} \pm (833 - 1250)$ Hz. The signal is sent to two parallel lock-in amplifiers with separate gain control, which demodulate each of the two modulation frequencies, thereby essentially shifting $\nu_{Q,V}$ back to zero. To avoid that the Stokes Q and V spectra fall on top of the Stokes I spectrum, they have to be frequency shifted (heterodyned) into two separate free frequency ranges. The heterodyning is done by mixing the two signals from the lock-in amplifiers with suitable frequencies derived from the FTS 2.5 kHz sampling pulses.

Polarization calibration was performed by making a recording of the interferogram at full resolution with an achromatic polarizer in front of the FTS, making the beam 100% polarized (linear or circular). For the calibration of Stokes V, a Fresnel rhomb plus a Glan-Thompson prism was used, for Stokes Q the Glan-Thompson prism alone was used.

The compensation of the instrumental polarization was improved considerably in comparison with the previous FTS recordings by using an achromatic compensator (Harvey, 1985), which in an "anti-McMath" device effectively containing all the

reflections with the same angles of incidence as in the McMath telescope, but in reversed order and with orthogonal position angles, such that the original Stokes vector is restored. Although this system worked extraordinarily well, imperfections in the compensation may cause a small residual instrumental polarization (generally $<0.1\%$ in Stokes V, $<0.2\%$ in Stokes Q), which has always been checked for and eliminated in the reduction procedure by shifting the fractional polarization spectra, Q/I and V/I, such that the continuum polarization becomes zero, as described in Stenflo et al. (1984). The residual instrumental fractional polarization is spectrally flat (in contrast to the undivided Stokes Q and V), and the continuum polarization is not significant compared with the Zeeman-effect polarization in the lines.

3. Extracted Stokes profile parameters

In the present exploratory investigation we have selected the spectral region 5246 – 5251 Å with the three Fe I lines at 5247.06, 5250.22, and 5250.65 Å and the Cr I line at 5247.57 Å for detailed analysis. Their effective Landé factors are 2.0, 3.0, 1.5, and 2.5, respectively. This region is well suited for the exploration of diagnostic problems, since it contains not only the line-ratio pair 5247.06 – 5250.22 Å for determinations of intrinsic field strengths in the fluxtubes, but also because the other two lines have a quite different temperature sensitivity, which permits diagnostics of the thermodynamic properties of the fluxtubes. The insight we gain from an exploration of this spectral region will then serve as a foundation for later attempts to apply a statistical approach using the properties of a large number of simultaneously observed line profiles.

To study the center-to-limb behavior of these spectral lines, we have extracted the following Stokes profile parameters with error bars: The amplitudes and areas of the Stokes V σ components, the amplitudes of the Stokes Q σ and π components, the wavelength position of the two Stokes V peaks, the wavelength position of the Stokes V zero-crossing, the wavelength position and half width of the Stokes I profile. From these basic parameters, determined in all the four lines of our selected region, various combinations of diagnostic interest have been formed, as will be seen in the next section.

The amplitudes of the two Stokes V σ components in the blue and red line wings were determined through parabolic fitting of the three highest points. The absolute values of the two amplitudes are denoted a_b and a_r, respectively. In the following, we define $V_{\max}$, the V amplitude of a line, as $0.5(a_b + a_r)$. If the magnetic field were vertical, $V_{\max}/\mu$ would be proportional to the filling factor α. The absolute values of the areas of the blue and red Stokes V peaks, A_b and A_r, were determined by simple trapezoidal integration.

As the Stokes Q spectra were much noisier than the Stokes V spectra, the procedure of using a parabolic fit to the highest three points was not adequate for the determination of the amplitudes of the Stokes Q σ and π components. Instead the numerically more stable procedure of fitting the whole profile through a non-linear least squares technique was chosen. As input reference profile for this fit we selected the most noise-free Stokes Q profile (one for each of the four lines) of our recordings, and let its two positive σ components and its negative π component be independently scaled to fit the other profiles. The procedure thus used three free scaling parameters, the fitted values of which gave the three desired amplitudes. We denote their absolute values by a_{σ_1}, a_{σ_2}, and a_π. As we do not find any significant asymmetry between a_{σ_1} and a_{σ_2}, we will in the following only use their sum: $a_\sigma = a_{\sigma_1} + a_{\sigma_2}$. In analogy with $V_{\max}$, we will also use the notation $Q_{\max}$ for the average amplitude of the Stokes Q σ components: $Q_{\max} = 0.5a_\sigma$.

The wavelength positions of the blue and red Stokes V peaks, λ_{V_b} and λ_{V_r}, were determined as the center of gravity of the part of the V profile above the level half-ways between the zero line and the peak value. Similarly, the wavelength position λ_I of the Stokes I profile was defined as the center of gravity of the part of the profile below the half level chord. It is convenient to express the width of the half level chord in velocity units as the Doppler width of a Gaussian that has the same half width as the measured I profile. Following the notation of Stenflo and Lindegren (1977), we denote this width v_D. The wavelength position of the Stokes V zero-crossing wavelength, determined directly from the V profile through interpolation, is denoted λ_V.

For all the above parameters error bars have been determined, through evaluating the standard deviations in the Stokes I and V recordings of the fluctuations in the continuous spectrum, and deriving how these errors propagate in the defining equations for the respective parameters. The error bars obtained thus represent *random* noise in the observations, but do not include possible (unidentified) systematic errors. Similarly, error bars for the various parameter combinations used in the next section were derived.

4. Results and their diagnostic contents

4.1. Line ratio in the Stokes V and Q amplitudes

It is natural to begin the exploration by considering the center-to-limb variation in the 5247.06 – 5250.22 line ratio of the amplitudes of V and Q. This line ratio, which has played a major role for our knowledge of the intrinsic field strengths in the spatially unresolved magnetic fluxtubes since it was introduced (Stenflo, 1973), has also been applied in the analysis of FTS Stokes V data obtained near disk center (Stenflo and Harvey, 1985; cf. also reviews by Stenflo, 1984, 1985b, 1986). The center-to-limb dependence of this line ratio would allow a determination of the height variation of the field strength in the fluxtube interior, i.e., the divergence of the field and the fluxtube geometry.

Although the μ-dependence of this line ratio has been measured (e.g. Frazier and Stenflo, 1978), the measurements have not been previously analyzed. The μ-dependence of other line ratios has been discussed (e.g. Howard and Stenflo, 1972; Frazier and Stenflo, 1972; Gopasyuk et al., 1973), but none of these ratios have the clean diagnostic potential of 5250 and 5247.

The physical basis of the line-ratio technique, which has previously only been applied to Stokes V data, is the non-linear relation between magnetic flux and amount of polarization when the Zeeman splitting is no longer small in comparison with the line width. As the deviation from linearity is different for lines of different Landé factor, it can be obtained from the line ratio, independently of the amount of flux or the filling factor of the observed region. This non-linearity or Zeeman saturation also occurs for Stokes Q, with different scaling, although the effect is more difficult to observe, since the Q signal is weaker and thus more affected by noise.

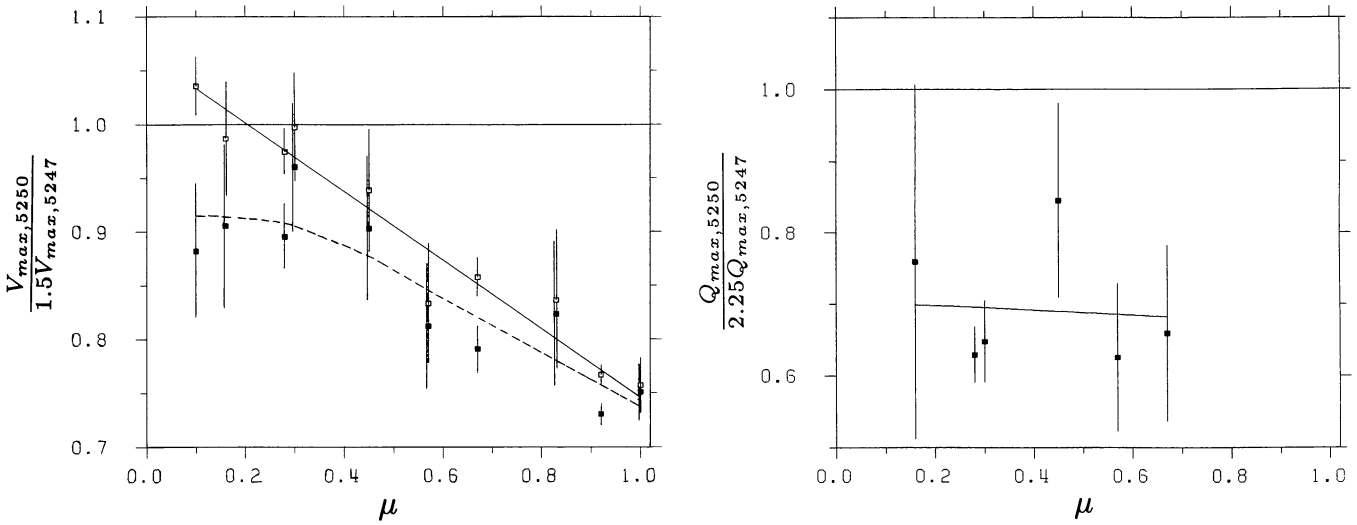

Fig. 2. Left diagram: Center-to-limb variation of the 5250.22 – 5247.06 line ratio of the Stokes V amplitudes. Filled squares and dashed curve (cubic spline fit): Directly determined line ratio. Open squares and solid line: Line ratio reduced to the case of zero filling factor, using the regression model of Eq. (1.1). Right diagram: 5250.22 – 5247.06 line ratio of the Stokes Q amplitudes (the solid line is a cubic spline fit)

If the magnetic fields were intrinsically weak (less than a few hundred G), the deviations from linearity between flux and polarization become insignificant. Then, using the definitions of the previous section for the maximum V and Q amplitudes, $V_{\max,5250} = 1.5V_{\max,5247}$ and $Q_{\max,5250} = 2.25Q_{\max,5247}$ (cf. Stenflo, 1985b). The factor 1.5 is the ratio g_{5250}/g_{5247} of the effective Landé factors of the two lines, the factor 2.25 is the square of this ratio (since for weak fields Stokes Q scales with the square of the Zeeman splitting, in contrast to the linear dependence of Stokes V).

The line ratios $V_{\max,5250}/(1.5V_{\max,5247})$ and $Q_{\max,5250}/(2.25Q_{\max,5247})$ should thus be unity for weak fields, but less than unity for intrinsically strong fields (due to more saturation in the polarization signal for the line with the larger Landé factor, i.e., the 5250 Å line). From the magnitude of the deviation from unity of the line ratio, the value of the field strength can be deduced.

Both the V and Q line ratios should be relatively insensitive to the actual inclination of the field vector, since the saturation effect that we are concerned with is determined by the amount of splitting, caused by the *absolute* field strength, whereas both the inclination and the filling factor determine the amount of polarization observed, i.e., the polarization scale. Since this scale is the same for both lines, it divides out when forming the line ratio, and only the saturation effect (the non-linearity) remains.

In Fig. 2 the directly observed Stokes V and Q line ratios are plotted as the filled squares. Both line ratios lie systematically well below unity, as a result of the strong-field (~kG) nature of the field. As expected, the Q ratio is much noisier than the V ratio, and hardly admits conclusions concerning its center-to-limb variation. Because of the extreme weakness of Stokes Q near disk center, the Q profiles could not be reliably evaluated in the recording at $\mu = 0.83$. The other two recordings near disk center, at $\mu = 0.92$ and 1.00, did not contain Q (they were the ones from 1979). Also the recording closest to the limb ($\mu = 0.10$) was too noisy to allow Q to be evaluated. Thus the Q results in Fig. 2 as well as in all the following diagrams only contain data representing 6 μ positions.

We therefore focus our attention on the V ratio. The observed values approach unity when going towards the limb, in qualitative agreement with previous studies of line ratio μ-dependence. This can be understood as a result of a decrease of the fluxtube field strength with height, as expected when the field lines spread out as the ambient gas pressure decreases exponentially.

Here it must be remembered, however, that the line ratio depends not only on the center-to-limb parameter μ, but also on the filling factor α, as demonstrated by Stenflo and Harvey (1985). In fact much of the scatter of the points around the dashed curve in Fig. 2, which is a cubic spline fit to the filled squares, is not due to noise but to the highly different filling factors of the regions sampled. This can be seen by making a qualitative comparison between the fluctuations in Fig. 2 with those of Fig. 1, which reflect the variations in the filling factor. As seen from the $V_{\max,5250}/\mu$ diagram of Fig. 1, we are subject to a selection effect such that the regions closer to the limb generally have a larger filling factor. As the line ratio decreases (field strength increases) with increasing filling factor (Stenflo and Harvey, 1985), the dashed curve in Fig. 2 tends to underestimate the height gradient of the field strength.

Due to the poor statistical coverage of the $\mu - \alpha$ plane in our observations, we cannot properly separate out these two dependencies. However, to provide a hint of what a correction for the filling-factor dependence would bring, we have tried to model the dependence of the line ratio of μ and α using a regression equation, assuming that the dependencies on both μ and $V_{\max,5250}/\mu$ (which is a poor but for the present purpose sensible substitute of the filling factor) are linear:

$$\frac{V_{\max,5250}}{1.5V_{\max,5247}} = c_0 + (c_1 + c_2\mu)(1 + c_3 V_{\max,5250}/\mu), \qquad (1.1)$$

where $c_{0,1,2,3}$ are the four free parameters to be determined by the regression.

After having applied this equation to fit the data, we can use the obtained coefficients to reduce the observed values to the case of zero filling factor. This procedure results in the open

squares and the solid straight line in the left diagram of Fig. 2. Similarly one can reduce the data to the disk center, plotting them as a function of $V_{\max,5250}/\mu$. Inspection of such a plot reveals that for large $V_{\max,5250}/\mu$ values (in particular at $\mu = 0.10$) the linear regression model vastly overestimates the filling-factor effect and gives unphysically low line ratios (that cannot be fit by any field strength). One reason for this overestimate is that $V_{\max,5250}/\mu$ is not proportional to the filling factor α since the magnetic field is not vertical, as will be evidenced by the Q/V ratio in Fig. 8. In principle one could use the information from the Q/V ratio in combination with $V_{\max,5250}$ to obtain a real estimate of the filling factor, taking the actually derived field direction into account, but we feel that for our present purposes such a sophistication is not warranted, since the form of the regression equation is rather *ad hoc* anyway, and it cannot be tested empirically due to our poor statistical coverage of the $\mu - \alpha$ plane.

Instead we consider the straight regression line in Fig. 2 as a kind of upper limit to the true relation that represents vanishing filling factor, since the filling-factor effect has been greatly exaggerated in deriving this line, in particular for small values of μ. Actually we rather believe that the dashed curve is a closer approximation of this relation than the solid line. In any case the two curves do not differ greatly from each other except close to the limb, for $\mu \lesssim 0.35$. Because of such problems of applying a regression equation, and since the filling-factor effects are anyhow relatively small as compared with the center-to-limb variations, we have refrained from trying to correct for the filling factor in the remaining diagrams of the present paper.

4.2. *Line ratio for the separation of the Stokes V peaks*

Another indicator of the intrinsic field strength is the wavelength separation between the Stokes V red and blue peaks, $\lambda_{V_r} - \lambda_{V_b}$. Since for weak magnetic fields Stokes V is simply proportional to $\partial I/\partial\lambda$, the V peak separation should equal the separation between the two inflexion points of the Stokes I profile. However, when the Zeeman splitting is no longer small as compared with the line width, the shape of V starts to deviate from that of $\partial I/\partial\lambda$, and the V peak separation increases in comparison with the Stokes I line width. This non-linearity, which causes Zeeman line broadening, contains information on the intrinsic field strength in the fluxtubes. In principle one could derive a field strength in this way from observations of a single spectral line, but in practice, as we will see below, only the line ratio technique gives results uncontaminated by other effects even in this case.

When plotting the observed separation of the Stokes V peaks vs. μ as in Fig. 3, we find that it increases rapidly towards the limb, both for the 5250 and 5247 Å lines. If this increase were due to Zeeman broadening, it would imply that the field strength increases rapidly with height, which is not plausible. The diagram to the right of Fig. 3, giving the width v_D of Stokes I in velocity units, shows however that most of the increase is simply an effect of a corresponding increase in the non-magnetic line width.

Accordingly the V peak separation should be normalized to the corresponding Stokes I line width to bring out the Zeeman broadening effect. This has been done in the left diagram of Fig. 4, where $\lambda_{V_r} - \lambda_{V_b}$ has been divided by the Stokes I line width, which has been defined as the measured half width multiplied by a factor that makes it equal to the separation between the inflexion points of a Gaussian with the same half width as the observed Stokes I. With this definition we would expect this ratio to be about unity if the fields were weak.

Figure 4 shows that this normalized Stokes V peak separation for the 5250 Å line decreases towards the limb, as expected when the field strength decreases with height. It is thus consistent with the line-ratio results of Fig. 2. For the 5247 Å line, the normalized V peak separation remains approximately independent of μ, which suggests that the Zeeman splitting is not large enough for the non-linear Zeeman broadening effects to become noticeable because of the smaller effective Landé factor (2.0) of this line. This indicates that the weak-field approximation is useful for the 5247 Å line. The reason why the mean level of the points is not unity as expected in the weak-field case has to do with the normalization procedure, which uses the observed Stokes I profile that does not originate from the same area as the Stokes V profile, as will be clarified next.

In fact most of the large scatter of the points in the diagram is of solar origin and directly related to the normalization in

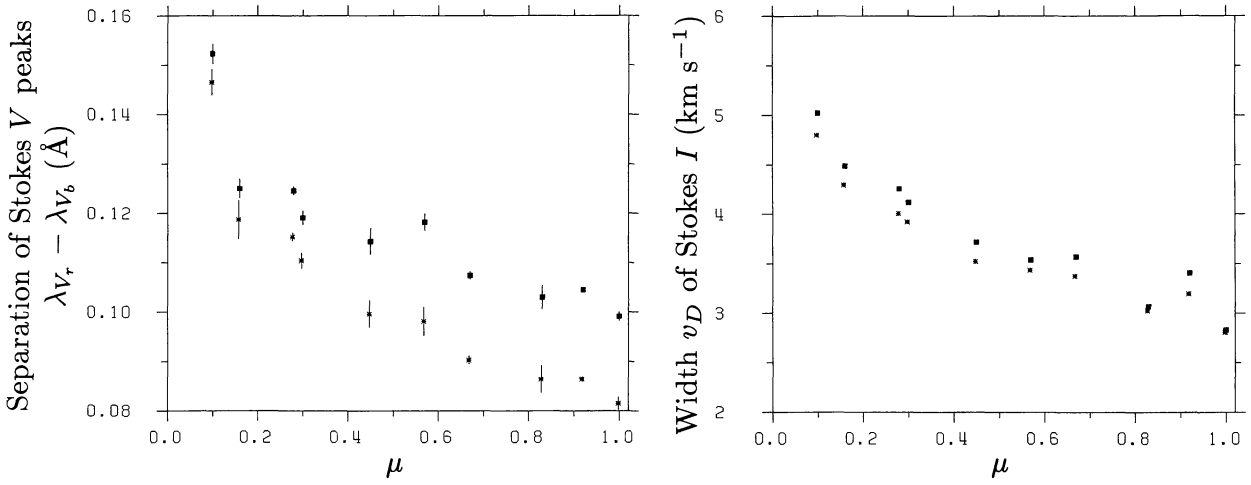

Fig. 3. Left diagram: Center-to-limb variation of the separation $\lambda_{V_r} - \lambda_{V_b}$ between the Stokes V peaks in the red and blue wings of the 5250.22 (filled squares) and 5247.06 (stars) Å lines. Right diagram: Center-to-limb variation of the width v_D of the corresponding Stokes I profiles, expressed in velocity units (as defined in Sect. 3)

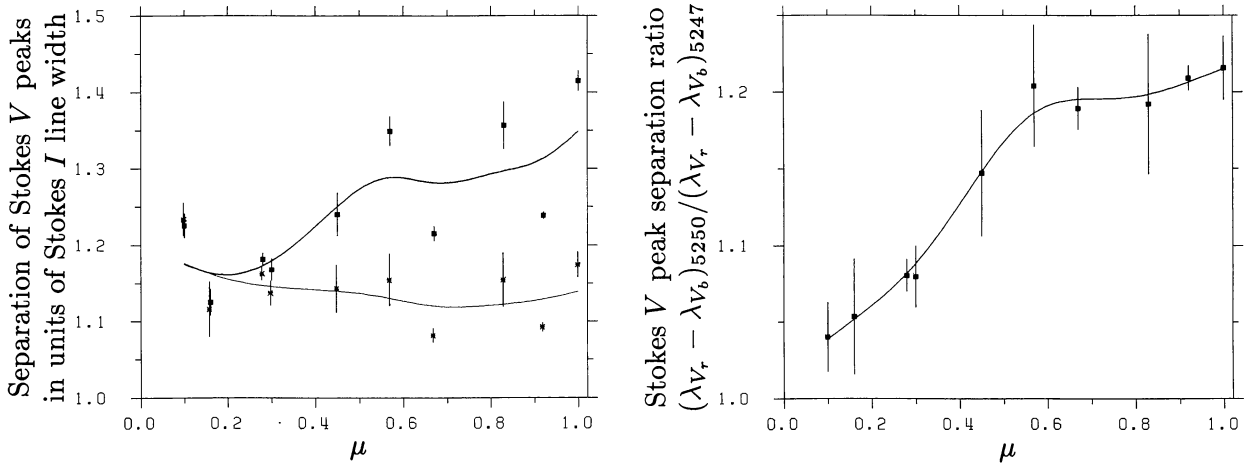

Fig. 4. Left diagram: Center-to-limb variation of the separation between the Stokes V peaks, normalized by dividing the values of the left and right diagrams of Fig. 3 with each other, after v_D has first been multiplied by a factor to make it represent the separation between the inflexion points of the profile (see text), for the 5250.22 (filled squares and thick curve) and the 5247.06 (stars and thin curve) Å lines. The curves are cubic spline fits. Right diagram: Line ratio $(\lambda_{V_r} - \lambda_{V_b})_{5250}/(\lambda_{V_r} - \lambda_{V_b})_{5247}$ of the Stokes V peak separation. The curve is a cubic spline fit

terms of the width of Stokes I. The problem is that whereas Stokes V exclusively originates from the small fraction of the resolution element occupied by magnetic fields (the filling factor), the whole resolution element contributes to Stokes I. Due to the generally small filling factors Stokes I is then more representative of the non-magnetic exterior region of the fluxtubes. As the thermodynamic conditions and the motions are very different between fluxtube interior and exterior, the Stokes I that originates inside the fluxtubes (we call it I_V to distinguish it from the observed I), and which should have been used for a proper normalization of the V peak separation, is greatly different from the observed Stokes I.

It is to eliminate this dependence on thermodynamics and on using a Stokes I that is not representative of the fluxtubes that we again need to employ the line-ratio technique. Since the 5250 and 5247 Å lines belong to the same multiplet of Fe I, have the same line strengths and excitation potentials, but only differ in their Zeeman patterns, their non-magnetic Stokes I profiles are essentially identical and obviously affected by non-magnetic line broadening in the same way. By forming the ratio $(\lambda_{V_r} - \lambda_{V_b})_{5250}/(\lambda_{V_r} - \lambda_{V_b})_{5247}$, we obtain a parameter exclusively determined by the amount of Zeeman-induced line broadening, uncontaminated by radiation from the fluxtube exterior or by any normalization problems.

The results for this 5250 – 5247 line ratio are displayed in the diagram to the right in Fig. 4. Most of the scatter of the previous diagram has disappeared, and we have obtained a well-defined relation with a decrease of the line ratio towards unity as we move towards the solar limb, as expected for fluxtubes whose cross sections increase with height. This diagram provides clean information on the intrinsic field strength independent of the Stokes V and Q amplitude line ratios of Fig. 2. Any fluxtube model would be required to satisfy all three diagrams.

4.3. Stokes V line ratio as a diagnostic of thermal structure

The ratio between the Stokes V amplitudes in different spectral lines is generally dependent on the combined, mixed effects of fluxtube thermodynamics and Zeeman saturation (caused by the large Zeeman splitting). The 5250.22 – 5247.06 Å line ratio is ideal for diagnostics of the field strength, since both lines are equally affected by the thermodynamics. Therefore thermodynamic effects cancel when forming the ratio, whereby the remaining effect of the field strength becomes isolated. In this line ratio, almost all the Zeeman saturation (deviation from linearity of the response of the polarization to magnetic flux) comes from the 5250 Å line, whereas the 5247 Å line is much less affected, as indicated for instance by the absence of a μ dependence for the 5247 Å line in the left diagram of Fig. 4. Thus, when forming line ratios between the other lines in our selected spectral region, Zeeman saturation plays a subordinate role, and most of the variations we see are due to thermodynamic effects.

In Stenflo et al. (1984), a comparison between the Stokes V profiles of our 5247.06 – 5250.22 Å line pair and the profile of the neighbouring Fe I λ 5250.65 Å line showed that the latter line had a larger polarization amplitude in spite of its effective Landé factor being substantially smaller (1.5). The reason for this is that the 5250.65 Å line is much less sensitive to temperature effects (line weakening) due to the considerably higher excitation potential of its lower level (2.20 eV, as compared with 0.09 and 0.12 eV for the 5247.06 and 5250.22 Å lines). Forming the Stokes V amplitude line ratio between lines of different temperature sensitivity thus provides information on the thermodynamic properties of the fluxtube interiors (Landi Degl'Innocenti and Landolfi, 1982).

Ideally the lines in a line pair selected to isolate the thermodynamic properties should be formed in the same layers of the atmosphere, but respond differently to the thermodynamic structure. In practice, however, lines of different thermodynamic response are generally not formed in identical layers, but these effects can be minimized by selecting lines of the same element, ionization stage, and line strength. Although the four lines in our selected spectral region are not optimum for this type of study, they are useful for our present purpose of illustrating the diagnostic principle.

As before for Fig. 2, we define the Stokes V amplitude line ratio as $(g_2 V_{\max,1})/(g_1 V_{\max,2})$, where indices 1 and 2 refer to lines

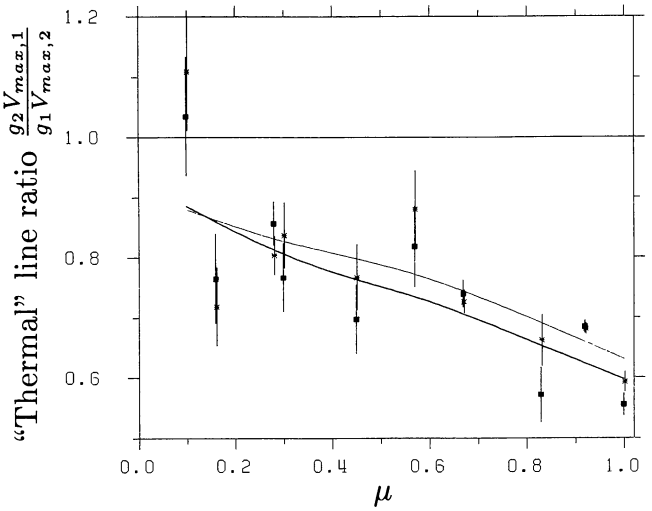

Fig. 5. Center-to-limb variation of the "thermal" line ratio $(g_2 V_{\max,1})/(g_1 V_{\max,2})$ between lines no. 1 and 2. Filled squares and thick curve: Line no. 1 is Fe I λ 5247.06 Å, line no. 2 is Fe I λ 5250.65 Å. Stars and thin curve: Line no. 1 is Cr I λ 5247.57 Å, line no. 2 is Fe I λ 5250.65 Å. The curves are cubic spline fits to the points

no. 1 and 2 in the pair. $g_{1,2}$ are the effective Landé factors. As the weak-field assumption is a good approximation when the 5250.22 Å line is excluded, $V_{\max}/g$ is proportional to the intensity gradient of the Stokes I profile I_V originating inside the fluxtubes, i.e., to $(\partial I_V/\partial\lambda)_{\max}$.

In Fig. 5 the filled squares and the thick curve give the results for the 5247.06 – 5250.65 Fe I line ratio, which according to the above represents $(\partial I_{V,5247.06}/\partial\lambda)_{\max}/(\partial I_{V,5250.65}/\partial\lambda)_{\max}$. Since the 5250.65 Å line is stronger than the 5247.06 Å line in the non-magnetic atmosphere, its $(\partial I/\partial\lambda)_{\max}$ is $\sim 13\%$ smaller at disk center (cf. Fig. 12 in Stenflo et al., 1984). Thus this line ratio is not expected to be unity in the absence of fluxtube effects, but ≈ 1.15 at disk center, and closer to unity near the limb. The circumstance that the observed line ratio lies far below unity is thus evidence for large differential line weakening, in the sense that the fluxtube interior is substantially hotter than the immediate surroundings at equal optical depth.

A straightforward interpretation of the increase of the line ratio towards unity when going towards the solar limb is that the temperature difference ΔT between fluxtube interior and exterior at equal optical depth *decreases* with height, in contradiction with most previous facular models (e.g. Chapman, 1979), but consistent with the model of Solanki (1984), which is based on an analysis of the FTS Stokes V data at disk center. This model requires ΔT to practically vanish at intermediate heights, slightly below the temperature minimum. We should however be cautious in making such a straightforward interpretation of Fig. 5, on account of the possible effects of fluxtube geometry when the fluxtubes are viewed obliquely (Van Ballegooijen, 1985).

The stars and the thin curve in Fig. 5 give the results for the Cr I 5247.57 – Fe I 5250.65 line ratio, which according to the above is representative of $(\partial I_{V,5247.57}/\partial\lambda)_{\max}/(\partial I_{V,5250.65}/\partial\lambda)_{\max}$. As these two lines are equally strong in the non-magnetic atmosphere, the line ratio should be close to unity in the absence of fluxtube effects. The results for this line ratio are very similar to those for the 5247.06 – 5250.65 line ratio showing the same relative center-to-limb variation, although the points lie slightly higher in the diagram. This small separation would become larger if we would normalize the curves to the corresponding non-magnetic $\partial I/\partial\lambda$ ratio. Thus, although the Cr I line is more temperature weakened than the Fe I 5250.65 line, it is less weakened than the Fe I 5247.06 line. Still it is surprising that its weakening is so large, since the excitation potential of its lower level is as high as 3.31 eV. However, as we are comparing lines of two different elements, the excitation potential is not the only variable determining the differential temperature weakening. Numerical radiative-transfer calculations are needed to clarify the differential behavior of lines of different chemical elements. Figure 5, however, serves to illustrate the considerable diagnostic potential of the "thermal" line ratio for determinations of the temperature structure of the fluxtubes.

4.4. *Stokes V asymmetries*

We define the relative Stokes V area asymmetry as $(A_b - A_r)/(A_b + A_r)$ and the relative Stokes V amplitude asymmetry as $(a_b - a_r)/(a_b + a_r)$, where $A_{b,r}$ and $a_{b,r}$ are the areas and amplitudes (absolute values) of the blue and red Stokes V peaks, as defined in Sect. 3. Their center-to-limb variations are plotted in Fig. 6.

In the case of the area asymmetry the values for the 5250.22 and 5247.06 Å lines closely agree with each other as well as with the Fe I 5250.65 and Cr I 5247.57 Å lines (not plotted in the figure to avoid cluttering the diagram). Curiously, the area asymmetry reverses sign around $\mu \approx 0.4$, from positive near disk center it becomes negative near the limb.

When inspecting the plot of the amplitude asymmetry in the right diagram of Fig. 6, we notice a considerable discrepancy between the results for the 5250.22 and 5247.06 Å lines. For this reason in this case also we have plotted the results for the two other lines to demonstrate that they agree well with 5250.22, but disagree with 5247.06. On account of this internal agreement between three of the four lines, we trust the solid curve (cubic spline fit) for the 5250.22 data as being representative of the behavior of the V amplitude asymmetry. Thus as concerns the amplitude asymmetry, there seems to be something anomalous with the 5247.06 Å line, the source of which we have not been able to identify. Let us however point out that the determination of the area asymmetry is numerically more stable than the amplitude asymmetry, since the integration makes use of essentially the full profile, whereas the amplitudes are determined from only the three points around the maximum (cf. Sect. 3).

Disregarding the anomalous 5247.06 Å line, the amplitude asymmetry remains positive near disk center, out to $\mu \approx 0.4$, where it drops to zero. This vanishing of the amplitude asymmetry occurs at about the same μ position where the sign reversal of the area asymmetry occured.

These asymmetries imply the existence of large internal mass motions inside the fluxtubes. Kemp et al. (1984) and Landi Degl'Innocenti (1985) have proposed an alternative mechanism involving asymmetrical optical pumping of the m sublevels rather than mass motions. Convincing arguments that the asymmetries are in fact due to internal mass motions come from the fact that the observed non-thermal broadening of the Stokes V profiles shows the same dependence on line strength and excitation potential as the asymmetries, indicating a common source (Solanki, 1985, 1986).

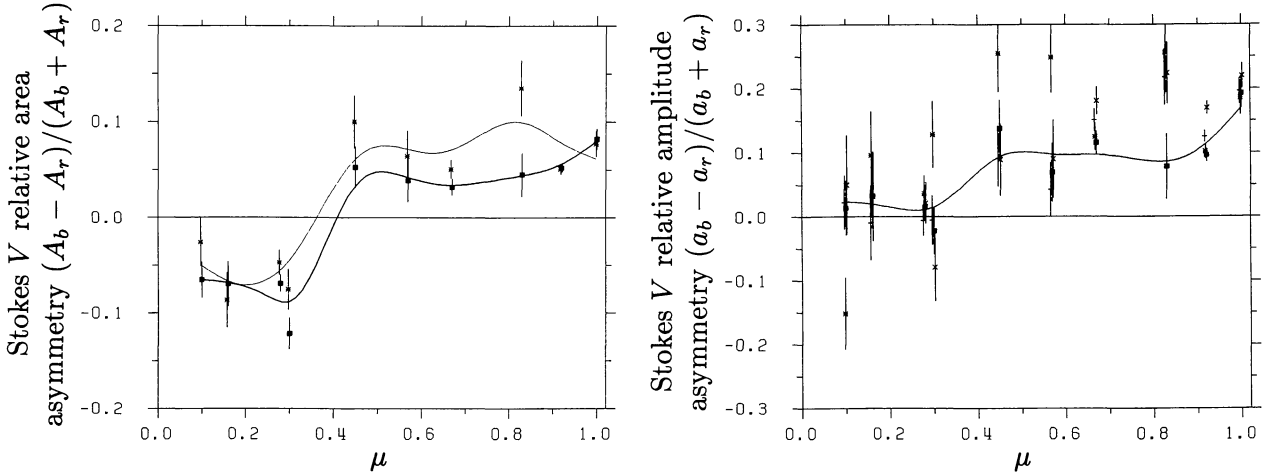

Fig. 6. Center-to-limb variations of the Stokes V relative area (left diagram) and amplitude (right diagram) asymmetries, for the 5250.22 (filled squares and thick curves), 5247.06 (stars and thin curve of the left diagram), Fe I 5250.65 (crosses), and Cr I 5247.57 (pluses) Å lines

For the Stokes V asymmetries to arise from the mass motions, there has to be a correlation between the corresponding Doppler shifts and the Zeeman splitting. In the case of the amplitude asymmetry, a lateral spatial correlation across the area inside the resolution element would be sufficient, but this could not generate any area asymmetry. Only line-of-sight gradients of the Doppler velocity in the fluxtubes are able to produce the Stokes V area asymmetry.

The decrease of the amplitude asymmetry when going towards the solar limb indicates that the responsible internal fluxtube mass motions are largely vertical, such that the line-of-sight component vanishes near the limb. Such a result is natural if the flow has to follow the field lines. The peculiar sign reversal of the area asymmetry on the other hand indicates some remarkable property in the line-of-sight correlations between the magnetic and velocity fields across the fluxtube (when we are not looking down along the fluxtube axis). The presence of an area asymmetry all the way to the limb may for example be due to the fact that the fluxtubes are embedded in the intergranular lanes, and the line of sight crossing the fluxtube at small values of μ will also sample the non-magnetic velocity field of the surroundings. Detailed modelling and radiative-transfer treatment may be needed to properly interpret this behavior.

4.5. *Stokes V Doppler shifts*

If there are mass motions inside the fluxtubes, it is natural to expect that the Stokes V profile as a whole should also be Doppler shifted. This is checked by plotting the wavelength position λ_V of the zero crossing of the Stokes V profile relative to the wavelength position λ_I (defined in Sect. 3) of the simultaneously observed Stokes I profile, i.e., the quantity $\lambda_V - \lambda_I$, which is displayed in Fig. 7 for the 5250.22 (filled squares) and the 5247.06 (stars) Å lines. The solid curve in the diagram may look like a cubic spline fit to the data, but this time it is not. Instead it represents the negative value of the *absolute* wavelength shift of the Stokes I profiles of the undisturbed, non-magnetic atmosphere, i.e., the difference between the observed and laboratory wavelengths, with the gravitational redshift and the relative motion between the observer and the solar region subtracted out. It has been derived from data presented in the thesis of Balthasar (1984). This absolute wavelength shift of Stokes I is primarily caused by the velocity-brightness correlation in the solar granulation. Since we use Stokes I as a reference for the Doppler shift of Stokes V, this curve in Fig. 7 represents the actual "zero level" to which the observed points should be referred in order to represent real net velocities and not only be an artifact of the granulation-induced shift of Stokes I.

Figure 7 shows that within the error limits, there are no significant net mass flows (no significant deviations from the Balthasar curve) for all center-to-limb distances (at least for $\mu \gtrsim 0.15$). The scatter of the points around the curve is typically $0.2\,\mathrm{km\,s^{-1}}$ (if we disregard the questionable observation at $\mu = 0.10$, 5 sec of arc from the limb). This is strong evidence for the absence of any systematic *net* mass flows inside the fluxtubes, in

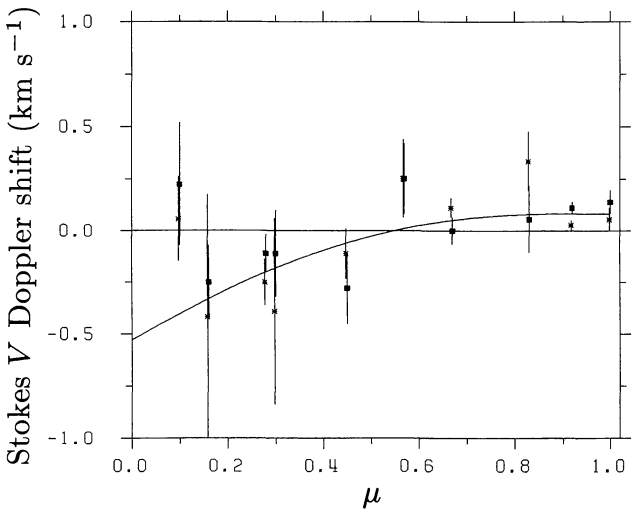

Fig. 7. Center-to-limb variation of the Doppler shift of the Stokes V zero crossing position relative to the position of the Stokes I profile, $\lambda_V - \lambda_I$, expressed in velocity units, for the 5250.22 (filled squares) and 5247.06 (stars) Å lines. The solid curve is the absolute wavelength shift with reversed sign of the non-magnetic Stokes I profile due to the velocity-brightness correlation in the solar granulation, derived from data of Balthasar (1984). It represents the corrected zero level for the Stokes V Doppler shifts

complete agreement with the conclusion of Stenflo and Harvey (1985) and with the detailed statistical analysis of 400 Fe I and 50 Fe II lines by Solanki (1986).

All models trying to explain the large Stokes V asymmetries with various forms of quasi-stationary flows also generate large ($>1\,\mathrm{km\,s^{-1}}$) shifts of the Stokes V zero-crossing wavelength λ_V (Pahlke and Solanki, 1986). The *simultaneous* observational constraints of large asymmetries, large non-thermal line broadenings, and no significant net Doppler shifts strongly suggest that the responsible fluxtube mass motions are basically non-stationary in nature (Stenflo, 1984, 1985b, 1986; Solanki, 1986). The most natural candidate mechanism seems to be fluxtube oscillations (e.g. Hasan, 1984; Venkatakrishnan, 1986), with the physical conditions in the up- and downmoving phases being different. Another proposed candidate mechanism is spicule ejection, with subsequent slower draining back of the plasma.

4.6. *Behavior of Stokes Q*

Since the Stokes Q recordings are considerably noisier than the corresponding Stokes V recordings and we could therefore only use six of the ten μ positions for the analysis as explained in Sect. 4.1, our treatment of the Stokes Q profiles will be much less thorough than in the case of Stokes V. Here we will limit ourselves to a discussion of the Stokes Q asymmetries and the Q/V ratio.

Although we find no significant amplitude asymmetry between the two σ components of the Stokes Q profiles, there is a very pronounced $\sigma - \pi$ amplitude asymmetry, as shown by the left diagram of Fig. 8. Here the asymmetry is defined as $(a_\sigma - a_\pi)/(a_\sigma + a_\pi)$, where a_σ is the sum of the amplitudes of the two σ components, and a_π is the amplitude with reversed sign (since the peak is normally negative) of the π component.

This $\sigma - \pi$ amplitude asymmetry provides information on the fluxtube intrinsic field strength, "orthogonal" in its diagnostic contents to the independent information provided by the Stokes V amplitude line ratio of Fig. 2 and the V peak separation line ratio of Fig. 4. If the Zeeman splitting of the line were complete, this Q asymmetry would in the optically thin case be zero. For reduced partial splitting, with increasing overlapping of the Zeeman components, the value of this asymmetry parameter should increase (Stenflo, 1985a). Figure 8, showing an increase towards the limb of the $\sigma - \pi$ asymmetry, is thus consistent with a height decrease of the intrinsic fluxtube field strength, as implied by Figs. 2 and 4. As however this asymmetry might also be affected by mass motions, one should be cautious in making a detailed interpretation.

When the inclination angle γ between the magnetic field vector and the line of sight changes, Stokes V scales as $\cos\gamma$, Stokes Q as $\sin^2\gamma$, almost independently of the amount of Zeeman splitting. We can express this by writing

$$\begin{aligned} Q &= q(B)\sin^2\gamma\,, \\ V &= v(B)\cos\gamma \end{aligned} \qquad (1.2)$$

(cf. Stenflo, 1985a). If we thus form the ratio $(Q\cos\gamma)/(V\sin^2\gamma)$, we obtain a function $(q(B)/v(B))$ dependent almost exclusively on the absolute value of the field strength B. For weak fields $q(B) \sim B^2$ whereas $v(B) \sim B$. For strong fields both functions saturate and become similar in magnitude (cf. Stenflo, 1985a, b). Thus the observed q/v ratio provides direct information on the intrinsic field strength. If for instance B decreases with height in the atmosphere, q/v would decrease when going towards the limb.

Unfortunately, however, it is not the q/v ratio that is the observed quantity, but Q/V. If we knew the field inclination γ, we could use (1.2) to directly transform Q/V into q/v, but γ cannot be obtained independently through other Stokes information. Instead, to derive γ one has to use the observed Q/V ratio supplemented by the information on the intrinsic fluxtube field strength B from e.g. the line ratio diagrams of Figs. 2 and 4.

Due to the strong buoyancy forces acting on the photospheric fluxtubes, we can expect that the field in isolated fluxtubes does not deviate much from the vertical direction. Very large inclinations to the vertical can however be expected in particular in young active regions, where strong fluxes of opposite polarity lie closely together, and the field has to bend over to connect with the other polarity. If, in our ignorance, we assume that the field is vertical, then $\cos\gamma/\sin^2\gamma = \mu/(1-\mu^2)$. Multiplying the Q/V ratio by this factor would then give us the field-strength function q/v.

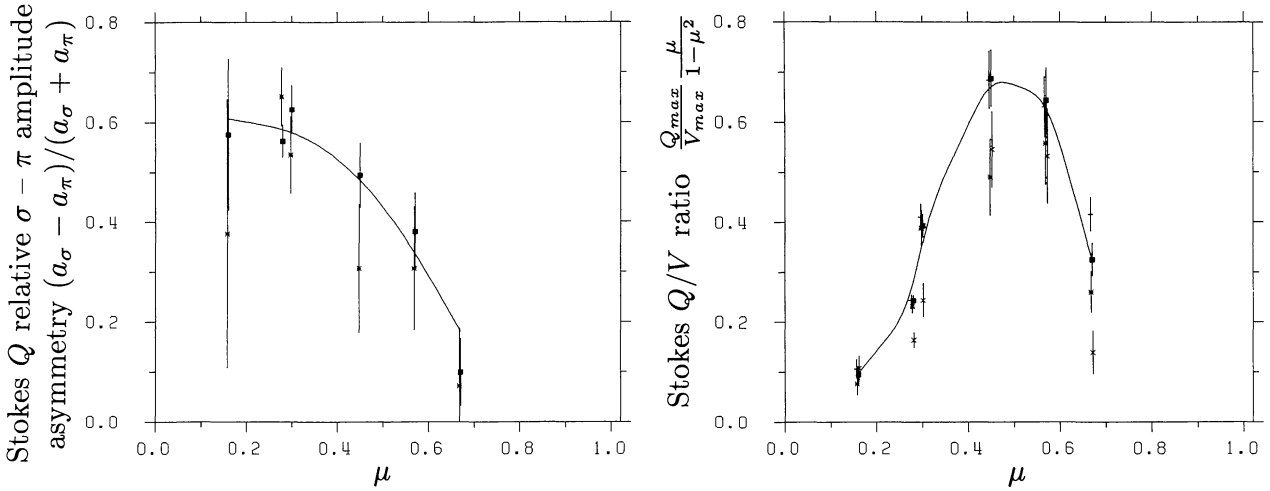

Fig. 8. Left diagram: Center-to-limb variation of the Stokes Q relative $\sigma - \pi$ amplitude asymmetry, as defined in text, for the 5250.22 (filled squares and solid line) and 5247.06 (stars) Å lines. Right diagram: Center-to-limb variation of $Q_{\max}\mu/[V_{\max}(1-\mu^2)]$, for the 5250.22 (filled squares and solid line), 5247.06 (stars), Fe I 5250.65 (crosses), and Cr I 5247.57 (pluses) Å lines. The curves are cubic spline fits

In the right diagram of Fig. 8 we have plotted $Q_{max}\mu/[V_{max}(1-\mu^2)]$, where Q_{max} and V_{max} are the averages of the amplitudes of the two σ components of Stokes Q and V, respectively, as defined in Sect. 3. The plot contains the results for all the four lines, to demonstrate that they all mutually agree. However, it is not possible to separate the effects of inclination and field strength from this diagram alone.

In Sect. 2 we explained how the procedure of finding a suitable magnetic region by centering on a local maximum in the Stokes V signal favored the selection of regions with a magnetic field tilted towards the observer rather than being vertical. This selection effect will decrease the Q/V ratio of Fig. 8, and will tend to be more pronounced close to the limb, where it was more difficult to achieve a good signal-to-noise ratio. The steep decline of the curve for small μ values in Fig. 8 may be at least partially due to this selection effect.

5. Conclusions

In the present paper we have tried to outline how new avenues of fluxtube diagnostics open up when making use of the center-to-limb variations of the Stokes spectra, and when including the linear polarization (Stokes Q) in the observations. The various profile parameters extracted are sensitive to different physical parameters inside the fluxtubes. Thus the intrinsic field strength is diagnosed primarily by the Stokes V and Q amplitude line ratios, the Stokes V peak separation line ratio, and the Stokes Q $\sigma-\pi$ relative amplitude asymmetry. Mass motions inside the fluxtubes are diagnosed by the Stokes V amplitude and area asymmetries and by the Doppler shift of the Stokes V zero-crossing wavelength. The fluxtube temperature structure can be diagnosed by the "thermal" Stokes V amplitude line ratio between lines of different temperature sensitivity and with insignificant Zeeman saturation. The field inclination can be derived from the Q/V amplitude ratio.

The center-to-limb variation of these various diagnostic tools provides the information needed to derive the height variation of these various fluxtube parameters, since the height of formation of the spectral lines varies with μ. However, a translation of this μ variation into a geometrical height scale requires extensive radiative-transfer calculations with fluxtube models, using lines of sight that cross the fluxtubes with their canopies at various oblique angles. The small-scale nature of the magnetic field makes this a complicated undertaking, but it is remarkable that it is at all possible to determine the MHD structure of the fluxtubes, considering the fact that their sizes are far smaller than can be spatially resolved by existing instrumentation.

A next step in the analysis of these recordings would be to use the statistical approach that has successfully been applied to the two recordings near disk center. Information on the height variations have been derived from the disk-center data by using the statistical dependences of the profile parameters on the line strength. Bringing in the center-to-limb variations will provide powerful new independent constraints on the possible height variations.

Due to our limited statistical sample of solar regions we have not been able to properly separate the effects of μ and filling-factor (α) dependence, although it appears that the center-to-limb dependence is the dominating factor. Future observations should aim at a better coverage of the $\mu-\alpha$ plane.

It would also be desirable to try to avoid the selection effect favoring regions with magnetic fields inclined towards the observer. This is difficult to do, however, without accompanying disadvantages like recording spectra with very weak signals, and introducing seeing and guiding noise by not having a magnetic feature centered within the FTS aperture during the long integration time. Due to these difficulties it may be better to maintain our present procedure, and use the observed Q/V ratio to determine the actual field inclination for each recording.

The use of the Q/V ratio to determine the field inclination however requires the assumption that the field vector lies in a plane containing the line of sight and the solar radius, which of course is not the case in general. For complete information on the field direction the fourth Stokes parameter, Stokes U, is needed. Hence there is a strong need to extend the FTS polarimeter scheme in future observations, to allow the simultaneous recording of all four Stokes parameters, I, Q, U, and V.

Acknowledgements. We are grateful to R. Hubbard for assistance in the operation of the FTS system, and to G. Ladd for carrying out the Fourier transforms and converting the data to user format. The work of one of us (S.K.S.) was supported by grants No. 2.814-0.83 and 2.666-0.85 from the Swiss National Science Foundation.

References

Balthasar, H.: 1984, Thesis, University of Göttingen
Brault, J.W.: 1978, *Oss. Mem. Astrofis. Arcetri* **106**, 33
Chapman, G.A.: 1979, *Astrophys. J.* **232**, 923
Frazier, E.N., Stenflo, J.O.: 1972, *Solar Phys.* **27**, 330
Frazier, E.N., Stenflo, J.O.: 1978, *Astron. Astrophys.* **70**, 789
Gopasyuk, S.I., Kotov, V.A., Severny, A.B., Tsap, T.T.: 1973, *Solar Phys.* **31**, 307
Harvey, J.W.: 1985, in M.J. Hagyard (ed.), *Measurements of Solar Vector Magnetic Fields*, NASA Conf. Publ. 2374, p. 109
Hasan, S.S.: 1984, *Astron. Astrophys.* **143**, 39
Howard, R., Stenflo, J.O.: 1972, *Solar Phys.* **22**, 402
Kemp, J.C., Macek, J.H., Nehring, F.W.: 1984, *Astrophys. J.* **278**, 863
Landi Degl'Innocenti, E.: 1985, in H.U. Schmidt (ed.), *Theoretical Problems in High Resolution Solar Physics*, MPA, Munich, p. 162
Landi Degl'Innocenti, E., Landolfi, M.: 1982, *Solar Phys.* **77**, 13
Pahlke, K.D., Solanki, S.K.: 1986, *Mitt. Astron. Ges.* **65**, 162
Solanki, S.K.: 1984, in T.D. Guyenne, J.J.Hunt (eds.), *The Hydromagnetics of the Sun*, ESA SP-220, p. 63
Solanki, S.K.: 1985, in H.U. Schmidt (ed.), *Theoretical Problems in High Resolution Solar Physics*, MPA, Munich, p. 172
Solanki, S.K.: 1986, *Astron. Astrophys.*, (in press)
Solanki, S.K., Stenflo, J.O.: 1984, *Astron. Astrophys.* **140**, 185
Solanki, S.K., Stenflo, J.O.: 1985, *Astron. Astrophys.* **148**, 123
Solanki, S.K., Stenflo, J.O.: 1986, *Astron. Astrophys.*, (in press)
Stenflo, J.O.: 1973, *Solar Phys.* **32**, 41
Stenflo, J.O.: 1976, in V. Bumba, J. Kleczek (eds.), *IAU Symp.* **71**, 69
Stenflo, J.O.: 1984, *Adv. Space Res.* **4**, 5
Stenflo, J.O.: 1985a, in M.J. Hagyard (ed.), *Measurements of Solar Vector Magnetic Fields*, NASA Conf. Publ. 2374, p. 263
Stenflo, J.O.: 1985b, *Solar Phys.* **100**, 189

Stenflo, J.O.: 1986, in *Proc. Workshop on Small Magnetic Flux Concentrations in the Solar Photosphere*, Göttingen, Oct. 1-3, 1985 (in press)
Stenflo, J.O., Harvey, J.W.: 1985, *Solar Phys.* **95**, 99
Stenflo, J.O., Harvey, J.W., Brault, J.W., Solanki, S.K.: 1984, *Astron. Astrophys.* **131**, 333
Stenflo, J.O., Lindegren, L: 1977, *Astron. Astrophys.* **59**, 367
Van Ballegooijen, A.A.: 1985, in M.J. Hagyard (ed.), *Measurements of Solar Vector Magnetic Fields*, NASA Conf. Publ. 2374, p. 322
Venkatakrishnan, P.: 1986, *Solar Phys.* **104**, 347